identical to each other and the two major forms of the activin-binding protein correspond to the 32- and 35-kD forms of follistatin.

To confirm this conclusion, we examined the effect of activin-binding protein on FSH release from cultured pituitary cells for follistatin-like activity (Fig. 4). The binding protein significantly suppressed FSH release in a concentration-dependent manner in the range of 0.4 to 100 ng/ml [median effective dose (ED_{50}), 5.2 ng/ml]. When compared with the concentration dependence of bovine inhibin, similar slope and maximal effect were obtained. However, the potency of the binding protein is 10 to 20% that of inhibin. This FSH suppression and activity ratio compared to inhibin is much like that reported for follistatin (*2, 19*). This supports the identity of the activin-binding protein and follistatin.

We obtained preliminary evidence that cultured rat ovarian granulosa cells produce activin-binding protein and secrete it into medium. We also purified an activin-binding protein from bovine pituitary that had the same chemical and biological characteristics as those of the binding protein from rat ovary (*20*). Together with various modulatory actions of activin on granulosa cells and pituitary cells, our findings support the idea that the binding protein may have an autocrine or paracrine function in the ovary and pituitary. Studies of the activin-binding protein from various cells may lead to a clearer understanding of the regulation of activin.

REFERENCES AND NOTES

1. D. M. Robertson *et al.*, *Biochem. Biophys. Res. Commun.* **126**, 220 (1985); K. Miyamoto *et al.*, *ibid.* **129**, 396 (1985); N. Ling *et al.*, *Proc. Natl. Acad. Sci. U.S.A.* **82**, 7217 (1985); J. Rivier, J. Spiess, R. McClintock, J. Vaughan, W. Vale, *Biochem. Biophys. Res. Commun.* **133**, 120 (1985); M. Fukuda *et al.*, *Mol. Cell. Endocrinol.* **44**, 55 (1986); D. M. Robertson *et al.*, *ibid.*, p. 271; L. J. Leversha *et al.*, *J. Endocrinol.* **113**, 213 (1987).
2. N. Ueno *et al.*, *Proc. Natl. Acad. Sci. U.S.A.* **84**, 8282 (1987); D. M. Robertson *et al.*, *Biochem. Biophys. Res. Commun.* **149**, 744 (1987).
3. W. Vale *et al.*, *Nature* **321**, 776 (1986); N. Ling *et al.*, *ibid.*, p. 779.
4. A. J. Mason *et al.*, *ibid.* **318**, 659 (1985); R. G. Forage *et al.*, *Proc. Natl. Acad. Sci. U.S.A.* **83**, 3091 (1986); A. J. Mason, H. D. Niall, P. H. Seeburg, *Biochem. Biophys. Res. Commun.* **135**, 957 (1986); F. S. Esch *et al.*, *Mol. Endocrinol.* **1**, 388 (1987); K. E. Mayo *et al.*, *Proc. Natl. Acad. Sci. U.S.A.* **83**, 5849 (1986); A. G. Stewart, H. M. Milborrow, J. M. Ring, C. E. Crowther, R. G. Forage, *FEBS Lett.* **206**, 329 (1986).
5. F. S. Esch *et al.*, *Mol. Endocrinol.* **1**, 849 (1987); S. Shimasaki *et al.*, *Proc. Natl. Acad. Sci. U.S.A.* **85**, 4218 (1988); S. Shimasaki *et al.*, *Mol. Endocrinol.* **3**, 651 (1989).
6. Y. Eto *et al.*, *Biochem. Biophys. Res. Commun.* **142**, 1095 (1987).
7. M. Murata, Y. Eto, H. Shibai, M. Sakai, M. Muramatsu, *Proc. Natl. Acad. Sci. U.S.A.* **85**, 2434 (1988).
8. H. Sugino *et al.*, *Biochem. Biophys. Res. Commun.* **153**, 281 (1988); Y. Hasegawa *et al.*, *ibid.* **156**, 668 (1988); L. A. Hutchinson, J. K. Findlay, F. L. de Vos, D. M. Robertson, *ibid.* **146**, 1405 (1987).
9. J. Yu *et al.*, *Nature* **330**, 765 (1987).
10. Y. Totsuka, M. Tabuchi, I. Kojima, H. Shibai, E. Ogata, *Biochem. Biophys. Res. Commun.* **156**, 335 (1988).
11. M. Kitaoka, I. Kojima, E. Ogata, *ibid.* **157**, 48 (1988).
12. H. Sugino *et al.*, *J. Biol. Chem.* **263**, 15249 (1988).
13. C. A. Campen and W. Vale, *Biochem. Biophys. Res. Commun.* **157**, 844 (1988); S. Kondo *et al.*, *ibid.* **161**, 1267 (1989); M. Hino *et al.*, *J. Biol. Chem.* **264**, 10309 (1989).
14. Immature female Wistar rats (21 to 23 days old) were injected subcutaneously with DES (2 mg in 0.1 ml of sesame oil) daily for 3 days. On day 4, eCG (50 IU) was injected subcutaneously. Two days after the injection of eCG, ovaries were obtained from rats killed by CO_2 inhalation. The organs were trimmed free of fat, frozen on dry ice, and stored at −85°C until use. This treatment augments the activin-binding activity in rat ovary by six to eight times greater than in nontreated rats.
15. After SDS-PAGE under nonreducing conditions, the gel was cut into 0.2-cm slices and the gel slices were placed overnight at 4°C in 1% Triton X-100 in 20 m*M* tris-HCl (*p*H 7.2) containing 150 m*M* NaCl and 0.1% bovine serum albumin (BSA). The activin-binding activity of the extracts was determined by the binding assay as described in the legend to Fig. 3.
16. Incubation of the activin-binding protein with 1.5 ng of ^{125}I-activin and increasing amounts of unlabeled activin resulted in progressive inhibition of the tracer binding; at 0.1 μg/ml the competition was 100%. In contrast, in the presence of inhibin, TGF-β, FSH, or LH at 10 μg/ml, the inhibition was less than 20%.
17. P. Matsudaira, *J. Biol. Chem.* **262**, 10035 (1987).
18. The third and thirteenth residues are deduced to be Cys by cDNA cloning analysis.
19. S.-Y. Ying *et al.*, *Biochem. Biophys. Res. Commun.* **149**, 133 (1987).
20. T. Nakamura and H. Sugino, unpublished observations.
21. M. Murata, K. Onomichi, Y. Eto, H. Shibai, M. Muramatsu, *Biochem. Biophys. Res. Commun.* **151**, 230 (1988).
22. U. K. Laemmli, *Nature* **227**, 680 (1970).

23. We thank D. N. Ward and G. R. Bousfield for critical reading of the manuscript and providing eCG; M. Igarashi, Y. Hasegawa, and K. Miyamoto for the gift of bovine inhibin and helpful suggestions; and the National Institute of Arthritis, Diabetes, and Digestive and Kidney Disease (NIADDK) Pituitary Hormone Program for supply of rat FSH assay kit and rat FSH. This work was supported in part by grants from the Ministry of Education, Science and Culture, Japan.

30 August 1989; accepted 3 November 1989

Endocranial Features of *Australopithecus africanus* Revealed by 2- and 3-D Computed Tomography

GLENN C. CONROY,* MICHAEL W. VANNIER, PHILLIP V. TOBIAS

The earliest hominid from South Africa, *Australopithecus africanus*, is known from only six specimens in which accurate assessment of endocranial capacity and cranial venous outflow pattern can be obtained. This places a severe limit on a number of hypotheses concerning early hominid evolution, particularly those involving brain–body size relationships and adaptations of the circulatory system to evolving upright posture. Advances in high-resolution two- and three-dimensional computed tomography (CT) now allow the inclusion of another important specimen to this list, MLD 37/38 from Makapansgat. A new computer imaging technique is described that "reconstructs" the missing portions of the endocranial cavity in order to determine endocranial capacity. In addition, CT evaluation allows assessment of cranial venous outflow pattern even in cases where the endocranial cavity is completely filled with stone matrix. Results show that endocranial capacity in this specimen is less than originally proposed and also support the view that gracile and robust australopithecines evolved different cranial venous outflow patterns in response to upright postures.

BRAIN SIZE IS AN IMPORTANT BIOlogical parameter and its measurement should be as accurate as possible, particularly in problems involving allometric growth and brain-body relationships (*1*). Even though it has been more than 60 years since *Australopithecus africanus* was first described (*2*), endocranial capacity estimates for this earliest South African hominid species are still based on only six individuals (Taung, Sts 60, Sts 5, Sts 19, Sts 71, and MLD 37/38) (*3–8*). Endocranial capacity estimates for one of these specimens, MLD 37/38 from Makapansgat, have varied from 480 cm^3 (*3*) to 435 cm^3 (*4, 9*), a difference of approximately 10%. Obtaining a reliable estimate of endocranial capacity in MLD 37/38 is difficult for two reasons: the endocranial cavity is filled with stone matrix, and part of the cranium anterior to the coronal suture is missing (Fig. 1). It would be impossible to extract the natural endocast intact from the calvaria; even to remove it

G. C. Conroy, Department of Anatomy and Neurobiology and Department of Anthropology, Washington University Medical School, St. Louis, MO 63110.
M. W. Vannier, Mallinckrodt Institute of Radiology, Washington University Medical School, St. Louis, MO 63110.
P. V. Tobias, Department of Anatomy and Human Biology, University of the Witwatersrand Medical School, Johannesburg, 2193, South Africa.

*To whom correspondence should be addressed.

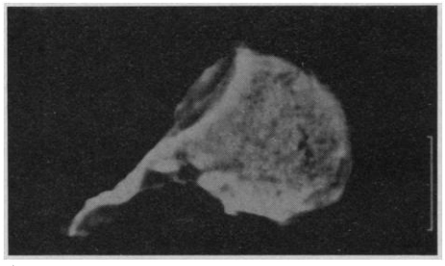

Fig. 1. Lateral view of MLD 37/38 (topogram). Note the missing frontal cortex anterior to the coronal suture. Scale bar, 5 cm.

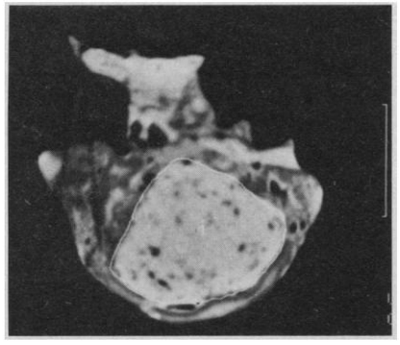

Fig. 2. Transaxial (2-mm) CT scan of MLD 37/38. Endocranial volume of this slice is 6.91 cm^3 (calculated by multiplying the area of ROI 1 (34.54 cm^2) by slice thickness (0.2 cm). Scale bar, 5 cm.

piecemeal would be difficult and risky and would be no guarantee of a clear-cut cleavage between the matrix and the endocranium. Any damage, however slight, to the endocranial surface would detract from the usefulness of preparing a silastic mold of the interior of the skull to produce an artificial endocast. Thus, paleoanthropologists face a catch-22 situation—a beautifully preserved, but unapproachable, endocranium.

Because direct endocranial volumetric determination was impossible on MLD 37/38, Dart (*3*) based his estimate on comparisons of external skull measurements between MLD 37/38 and Sts 5, an *A. africanus* skull from Sterkfontein. The endocranial capacity of this latter skull had been estimated at 482 cm^3 by Broom *et al.* (*10*), although they did not discuss how this figure was obtained. However, this value for Sts 5 was later confirmed by Holloway (*5, 9*).

However, Holloway's (*4*) estimate of endocranial volume in MLD 37/38 (435 cm^3) was about 10% less than that originally determined by Dart (*3*). Again, since direct measurement was impossible, he resorted to modifying a formula originally devised to measure endocranial volume in modern human skulls based on roentgenologic measurements (*11*) and then had to use a different specimen (the MLD 1 parieto-occipital fragment) to infer cranial thickness at the occipital pole, in the cerebellar fossa, and in

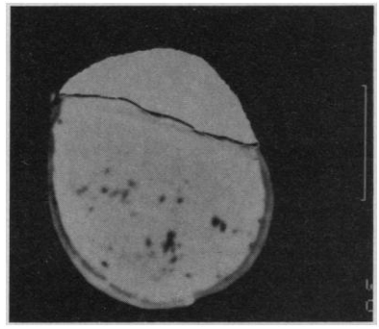

Fig. 3. "Opacified" reconstruction of portion of frontal cortex. Volume of this reconstructed portion is 3.48 cm^3 (17.42 cm^2 × 0.2 cm). Scale bar, 5 cm.

the temporal region. Although a pilot study showed that this method could predict endocranial capacity within a 2% error in modern pongid skulls, the results for MLD 37/38 (which has neither a modern human nor modern pongid-shaped calvaria) could not be confirmed by any independent test. Moreover, it was pointed out that MLD 1 probably belonged to a young adult male, whereas MLD 37/38 could have belonged to a young adult female (*7*). In spite of this, Holloway's conclusions have been accepted in all subsequent tabulations of early hominid endocranial capacity. Thus, in order to test the accuracy of Holloway's methods and to independently assess cranial capacity in MLD 37/38, the specimen was subjected to two- and three-dimensional computed tomography (CT) (*12–17*).

MLD 37/38 was CT-scanned in transaxial, coronal, and sagittal planes (*18*). The technique used to measure endocranial volume by CT is essentially that described by Conroy and Vannier (*13*). A new technique was developed in order to "reconstruct" missing portions of the MLD 37/38 skull. A total of 46 contiguous transaxial CT slices were used in this analysis from the foramen magnum to the top of the calvaria. As each 2-mm CT section was displayed on the Evaluscope's monitor, the stone matrix was distinguished from the overlying endocranial surface by level-slicing or thresholding techniques. An endocranial region of interest (ROI) was created by tracing the contour marking the interface of matrix and endocranium with the Evaluscope's built-in digitizer resistor pad and stylus. Once this ROI was established, the STATISTIC command calculated the area of the ROI in square centimeters. This area was multiplied by 0.2 cm (slice thickness) to give the endocranial slice volume in cubic centimeters. The endocranial volume of every slice was stored and summed to give a total endocranial volume of the preserved specimen (Fig. 2).

This procedure was straightforward for the first 23 CT slices. However, CT slices 24 to 46 traversed both the preserved and missing portions of the cranium. In each of these CT slices, the missing frontal cortex was reconstructed by drawing, and then "opacifying," it on the computer screen so that it formed a symmetrical fit with the preserved portion of the endocranium (Fig. 3). The volume of the reconstructed and preserved endocranial portions of each CT slice was calculated in the manner described above and recorded. Three-dimensional images were generated from the CT data in order to visually assess the accuracy of the reconstructed missing frontal cortex (Fig. 4).

The volume of the preserved and reconstructed endocranial cavity was 372 cm^3 and 53 cm^3 respectively, giving a total endocranial capacity of 425 cm^3. Thus, two independent lines of investigation now confirm that the cranial capacity of MLD 37/38 is at least 10% less than originally recorded by Dart. This is a reliable estimate since endocranial volume determination by CT is high-

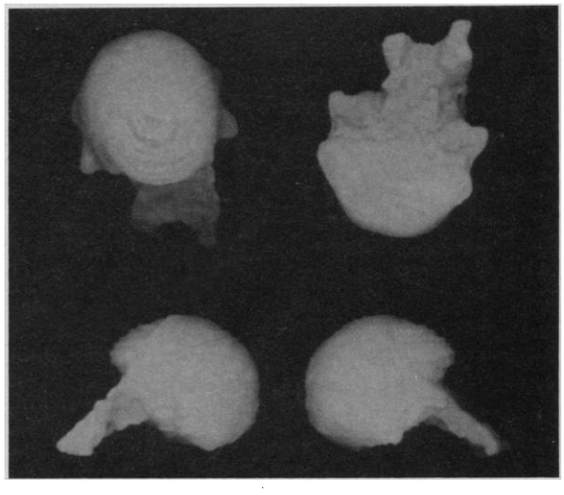

Fig. 4. Four three-dimensional reconstructions of MLD 37/38 (with "opacified" frontal cortex included) produced from sequential 2-mm transaxial CT scans. Upper left, top view; upper right, basal view; bottom left, left lateral view; bottom right, right lateral view.

ly accurate, even in primates of markedly different endocranial shapes (*13*). This is the lowest endocranial capacity estimate for any specimen of *A. africanus* to date. The other available values are Sts 60, 428 cm^3; Sts 71, 428 cm^3; Sts 19, 436 cm^3; Taung, 440 cm^3; and Sts 5, 485 cm^3 (*5*). The sample mean of endocranial capacity for *A. africanus* becomes 440.3 cm^3, which is slightly smaller than other recent estimates (*5, 7*).

Another important biological feature of early hominids is their pattern of cranial venous outflow. Australopithecine species often differ in the pattern of intracranial venous blood flow around the basioccipital region. An enlarged occipital-marginal sinus system is uncommon in *A. africanus* (as in modern *Homo sapiens*), but is common in *A. robustus*, *A. boisei*, and Hadar hominids usually designated *A. afarensis* (*19–24*). Although the reasons for this difference in frequency are obscure, it has been suggested that they may relate to factors involved with more efficient blood flow to the vertebral venous plexus in evolving bipedal hominids. In addition, these patterns are crucial to several phylogenetic hypotheses concerning early human evolution (*22, 23*).

Again, however, these observations are based on very limited sample sizes for early South African hominids. The presence or absence of enlarged occipital-marginal sinuses can be determined on only five individuals of *A. africanus* (Taung, Sts 5, Sts 19, Sts 26, and MLD 1). Of these, only the Taung individual shows occipital-marginal enlargement (*21*). In order to increase this sample size, we performed CT examination of the MLD 37/38 squama occipitalis to determine cranial venous outflow pattern in this *A. africanus* individual. Because of the small sample sizes involved, the results of this investigation impact significantly on phylogenetic and functional interpretations of cranial venous outflow patterns in early hominids (*21–24*).

The occipital examination of MLD 37/38 was based on contiguous 2-mm-thick CT scans taken in the coronal and transaxial planes. Anatomical detail was exquisitely preserved in the CT scans (Fig. 5). From CT experiments done on a cast of the occipital of OH 5 (*A. boisei*), enlarged marginal sinus grooves, if present, would be visible as shallow sulci on either side of the foramen magnum leading toward the jugular foramen. Coronal and transaxial CT scans through the posterior part of the cranium of MLD 37/38 clearly show a number of relevant anatomical features: internal occipital protuberance and crest, cerebellar fossae, petrous pyramids, foramen magnum, jugular foramen, well-developed sigmoid sinus grooves, and vermian fossa (Fig. 6). There is

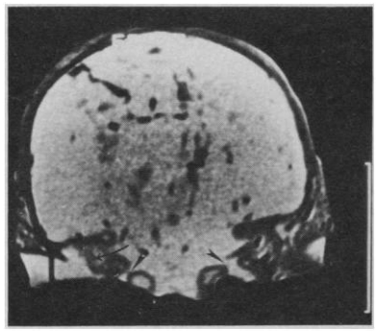

Fig. 5. Coronal CT scan (2 mm). Note the handle of the malleus in the right middle ear cavity (arrow) and the jugular canals bilaterally (arrowheads). Scale bar, 5 cm.

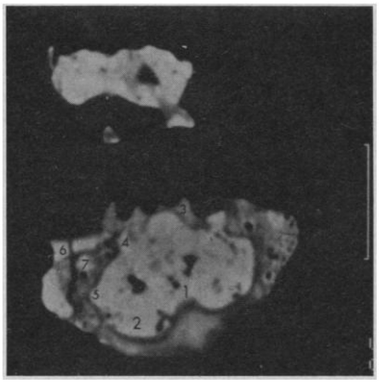

Fig. 6. Transaxial CT slice (2 mm). Note internal occipital crest (1), cerebellar fossae (2), basilar part of occipital bone (3), jugular foramen (4), groove for the sigmoid sinus (5), external acoustic meatus (6), petrous part of temporal bone (7). Scale bar, 5 cm.

no sign of a marginal sinus groove lateral to the flanking ridge of the vermian fossa, where it would be expected, and is indeed present, in *A. boisei* OH-5 ("Zinjanthropus"). In addition, although the internal occipital crest is clearly visualized, neither the occipital sinus groove, nor its flanking ridges can be seen throughout the relevant area. Grooves for the sigmoid sinus are clearly present and enlarged as they would be with transverse-sigmoid sinus drainage. It may thus be inferred that MLD 37/38 is like the crania of most other *A. africanus* in lacking an enlargement of the occipital-marginal sinuses and in depending for its venous drainage on the lateral sinus system (*25*).

Thus, of six *A. africanus* specimens in which enough of the area below the internal occipital protuberance is preserved for observation, the Taung skull remains the only one showing occipital-marginal sinus enlargement (*21*). This figure falls well below the values for Hadar, *A. boisei*, and *A. robustus*, but is comparable in order of magnitude to the frequencies in modern human populations. These data support the view that the Hadar hominids and robust australopithecines responded to realigned hydrostatic pressures of bipedalism by enlarging the occipital-marginal sinus system to increase blood flow to the vertebral venous plexus, whereas gracile australopithecines and *Homo* preferentially delivered blood to the vertebral venous plexus via extensive anastomotic channels (including emissary veins) around the foramen magnum (*22, 23*). The latter vascular arrangement may have been an evolving mechanism for cooling the enlarging brain in an *A. africanus*–early *Homo* lineage (*23*).

REFERENCES AND NOTES

1. M. D. Pagel and P. H. Harvey, *Science* **244**, 1589 (1989).
2. R. A. Dart, *Nature* **115**, 195 (1925).
3. ———, *Am. J. Phys. Anthropol.* **20**, 119 (1962).
4. R. L. Holloway, in *The Functional and Evolutionary Biology of Primates*, R. Tuttle, Ed. (Aldine-Atherton, New York, 1972), pp. 185–203.
5. ———, in *Primate Functional Morphology and Evolution*, R. Tuttle, Ed. (Mouton, The Hague, 1975), pp. 393–416.
6. P. V. Tobias, *The Brain in Hominid Evolution* (Columbia Univ. Press, New York, 1971).
7. ———, in *Primate Functional Morphology and Evolution*, R. Tuttle, Ed. (Mouton, The Hague, 1975), pp. 353–392.
8. ———, *J. Hum. Evol.* **16**, 741 (1987).
9. R. L. Holloway, *Science* **168**, 966 (1970).
10. R. Broom, J. T. Robinson, G. W. H. Schepers, *Transvaal Mus. Mem.* **4**, 11 (1950).
11. I. L. MacKinnon, J. A. Kennedy, T. V. Davies, *Am. J. Roentgenol. Radium Ther. Nucl. Med.* **76**, 303 (1956).
12. G. C. Conroy and M. W. Vannier, *Science* **226**, 456 (1984).
13. ———, in *Hominid Evolution: Past, Present and Future*, P. V. Tobias, Ed. (Liss, New York, 1985), pp. 419–426; L. A. Winkler, G. C. Conroy, M. W. Vannier, in *Orang-utan Biology*, J. H. Schwartz, Ed. (Oxford Univ. Press, Oxford, 1988), pp. 225–232.
14. G. C. Conroy and M. W. Vannier, in *Proceedings of the 10th International Primate Congress, Nairobi*, J. Else and P. Lee, Eds. (Cambridge Univ. Press, Cambridge, 1986), pp. 211–222.
15. M. W. Vannier, G. C. Conroy, J. L. Marsh, R. H. Knapp, *Am. J. Phys. Anthropol.* **67**, 299 (1985).
16. M. W. Vannier and G. C. Conroy, *Folia Primatol.* **53**, 7 (1989).
17. ———, *ibid.*, p. 22.
18. Contiguous nonoverlapping high-resolution CT scans were taken at a slice thickness of 2 mm with a Siemens DR3 CT scanner at the Department of Radiology, Hillbrow Hospital, Johannesburg. Extended bone range window settings were used since the fossilized skull and matrix were well beyond +1000 Hounsfield units (with the x-ray tube operated at 125 kVp), the upper limit of normal CT viewing. All CT scans and digital radiographs used for localization (topograms) were stored on 8-inch single-sided, double-density, floppy disks for transportation to the Mallinckrodt Institute of Radiology at Washington University Medical School where they were analyzed on a Siemens Evaluscope-DR reviewing console. Hard copies of all images were made with a Matrix Instruments MI-10 camera.
19. P. V. Tobias, *Olduvai Gorge* (Cambridge Univ. Press, Cambridge, 1967), vol. 2.
20. ———, in *Anthropologie und Humangenetik*, R. Peter, F. Schwartzfischer, G. Glowatzki, G. Ziegelmayer, Eds. (Fischer, Stuttgart, 1968), pp. 1–10.
21. ——— and D. Falk, *Am. J. Phys. Anthropol.* **76**, 309 (1988).
22. D. Falk and G. C. Conroy, *Nature* **306**, 779 (1983).
23. D. Falk, *Am. J. Phys. Anthropol.* **70**, 311 (1986); *Behav. Brain Sci.*, in press.

24. W. H. Kimbel, *Am. J. Phys. Anthropol.* **63**, 243 (1984).
25. F. W. Zonneveld and J. Wind, in *Hominid Evolution: Past, Present and Future*, P. V. Tobias, Ed. (Liss, New York, 1985), pp. 427–436; J. Wind and F. W. Zonneveld, *Naturwissenschaften* **76**, 325 (1989). These authors have noted the funnel-shaped external auditory meatus and the lateral semicircular canal-posterior clivus angle (30°) in MLD 37/38. This angle suggests to them that the neck was held about 20° less vertical than in modern man.

26. We thank the radiographers at Hillbrow Hospital, Johannesburg, particularly R. van der Riet, I. Amla, S. Ligarabe, F. Gora, and R. Harman. R. Knapp provided technical assistance at the Mallinckrodt Institute of Radiology. Supported by the National Science Foundation, the Council for International Exchange of Scholars, and the L. S. B. Leakey Foundation.

12 October 1989; accepted 21 December 1989

Genetic Analysis of Histone H4: Essential Role of Lysines Subject to Reversible Acetylation

PAUL C. MEGEE, BRIAN A. MORGAN, BARBARA A. MITTMAN,* M. MITCHELL SMITH†

The nucleosome is the fundamental unit of assembly of the chromosome and reversible modifications of the histones have been suggested to be important in many aspects of nucleosome function. The structure-function relations of the amino-terminal domain of yeast histone H4 were examined by the creation of directed point mutations. The four lysines subject to reversible acetylation were essential for histone function as the substitution of arginine or asparagine at these four positions was lethal. No single lysine residue was completely essential since arginine substitutions at each position were viable, although several of these mutants were slower in completing DNA replication. The simultaneous substitution of glutamine for the four lysine residues was viable but conferred several phenotypes including mating sterility, slow progression through the G_2/M period of the division cycle, and temperature-sensitive growth, as well as a prolonged period of DNA replication. These results provide genetic proof for the roles of the H4 amino-terminal domain lysines in gene expression, replication, and nuclear division.

THE NH_2-terminal domain of histone H4 has been highly conserved throughout evolution. The first 20 amino acids of yeast and mammalian histone H4 are identical, suggesting essential functions for this region of the protein. The NH_2-terminal domain includes the sites for a variety of posttranslational modifications including methylation, phosphorylation, and acetylation (*1*). In yeast, as in other eukaryotes, four lysine residues at positions 5, 8, 12, and 16 are subject to reversible acetylation at their ϵ-amino groups (*2*). Changes in lysine acetylation states have been correlated with the onset of a variety of nuclear functions, including transcription, replication, chromatin assembly, and spermatogenesis (*1, 3*). These acetylation changes are presumed to be critical in effecting the dynamic alterations of histone-DNA and histone-protein interactions required for function. Therefore, it is perhaps surprising that the wild-type yeast histone H4 genes can be replaced with alleles that lack the sequences encoding amino acids 4 to 28 (*4*) or 2 to 26 (*5*). Cells with these deletion alleles as their sole source of histone H4, though viable, suffer a variety of defects including a slower growth rate, derepression of the silent mating-type genes resulting in phenotypic sterility (*4, 5*), and temperature-sensitive growth (*5*).

One interpretation of the unexpected viability of the NH_2-terminal deletion mutants is that the four lysine residues do not provide an essential biological function and that changes in their acetylation states are merely coincidental. To test this hypothesis, an allele of the yeast histone H4 gene was constructed (*6*) in which all four lysine codons at amino acid positions 5, 8, 12, and 16 were changed to arginine codons (*hhf1-9*). The functions of this allele, as well as the others used in this study, were assayed by the complementation of histone gene deletions in yeast. The histone H3 and H4 genes in *Saccharomyces cerevisiae* are arranged as divergently transcribed gene pairs with one H3 gene and one H4 gene sharing a common promoter region. To avoid disrupting the normal regulation of the genes and to maintain the stoichiometry of H3 to H4 histone, we engineered all constructs as H3-H4 gene pairs. The haploid genome contains two nonallelic sets of H3-H4 gene pairs (*7*). The copy-I H3 (*HHT1*) and H4 (*HHF1*) genes make up the first set, while the copy-II H3 (*HHT2*) and H4 (*HHF2*) genes make up the second unlinked set. Either set of genes is sufficient for cell growth, but simultaneous deletion of both loci is lethal (*8*). The *hhf1-9* allele together with a wild-type histone H3 gene (*HHT1*) were used to complement deletions of both chromosomal gene sets by two different protocols (*9*). In the first procedure, we attempted to rescue a spore colony deleted for both chromosomal copies of the H3-H4 gene sets (Fig. 1A); such colonies are recognized by their nonsectoring white phenotype and sensitivity to 5-fluoroorotic acid (5-FOA). Although a control plasmid carrying the wild-type H4 gene could efficiently rescue the chromosomal deletion segregants, the *hhf1-9* allele failed to give viable colonies in both tetrad dissections and random spore screens. We also tested *hhf1-9* using a high copy number yeast vector in case it could provide minimal function at higher gene dosage. These derivatives also failed to give colonies.

To eliminate the possibility that *hhf1-9* was only defective in spore germination, we tested it in a "plasmid shuffle" assay (*10*) (Fig. 1B). A control plasmid containing the wild-type H4 gene produced colonies at high efficiency in this test, but the *hhf1-9* allele did not produce colonies, indicating that the mutant was not viable. Since cells carrying the *hhf1-9* allele grew normally in the presence of either a chromosomal or a plasmid copy of the wild-type H4 gene, the mutations in *hhf1-9* must confer a recessive loss of function rather than a dominant lethality. Thus, one or more of the lysine residues at positions 5, 8, 12, and 16 provide an essential function when the NH_2-terminal domain is present intact and cannot be mutated to arginine without the loss of this function.

These results suggested that the inviability of *hhf1-9* might be caused by the continuous presence of positively charged arginine side chains. According to this model, the presence of positive charges at positions 5, 8, 12, and 16 would be lethal at some stage of the cell cycle; in the wild-type gene, the charged lysine residues would be neutralized by acetylation, and in the NH_2-terminal deletion mutation, the positive charges would be missing completely. This model made two predictions: that replacement of the four lysines with unchanged amino acids would produce a viable phenotype, and that the mutant would mimic the behavior of the NH_2-terminal deletion mutants.

Department of Microbiology, School of Medicine, University of Virginia, Charlottesville, VA 22908.

*Present address: Department of Biology, University of Richmond, VA 23173.
†To whom correspondence should be addressed.